Philippine Journal of Science
148 (1): 63-72, March 2019
ISSN 0031 - 7683
Date Received: 24 Jul 2018

Photoheterotrophic Hydrogen Production of *Rhodobacter sphaeroides* KCTC 1434 under Alternating Ar and N_2 Headspace Gas

Ruby Lynn G. Ventura[1]*, **Jey-R S. Ventura**[2], and **Young-Sook Oh**[3]

[1]Rural High School, College of Arts and Science, University of the Philippines Los Baños, Paciano Rizal, Bay 4033 Laguna, Philippines
[2]Department of Engineering Science, College of Engineering and Agro-Industrial Technology, University of the Philippines Los Baños, College, Los Baños 4031 Laguna, Philippines
[3]Department of Environmental Engineering and Energy, Myongji University, 116 Myongji-Ro, Cheoin-Gu, Yongin, Gyeonggi-Do 449-728 Republic of Korea

In this paper, the effect of switching argon (Ar) and nitrogen (N_2) headspace gases during the onset of photofermentative H_2 production on butyrate and propionate was studied using *Rhodobacter sphaeroides* KCTC 1434. Reactor headspace were initially purged with N_2 in the first set-up, while Ar was used in the second set-up. After 60 h, the first set of reactors were repurged with N_2 (PN_2R, BN_2R); while the second set were replaced with Ar (PArR, BArR). Results showed that replacement with N_2 automatically decreased H_2 productivity in propionate and butyrate by 5.5 and 4.0 times, respectively. Replacement with N_2 led to changes in cell densities and increased final pH in the culture medium. On the other hand, initial exposure to N_2 and subsequent re-purging with Ar significantly increased ($p = 7.87 \times 10^{-10}$) cell weight and delayed entry of the strain to stationary phase of cell growth. H_2 production lag times were determined to be 144 h for PArR (Substrate conversion efficiency, SCE = 96.63%) and 172 h for BArR (SCE = 55.60%). Exposure to any of the gases did not bring significant difference in substrate consumption. Overall, the investigation showed that utilizing N_2-to-Ar headspace purging is feasible in photofermentation setup. Further exploration involving pH control and quantification of ammonia (NH_3) and polyhydroxybutyrate (PHB) may be carried to extend the use of this setup in a photofermentation system.

Keywords: biohydrogen production, photofermentation, reactor headspace gas, *Rhodobacter sphaeroides*

INTRODUCTION

The worldwide dependency on fossil fuel has created the aggravation of global warming by greenhouse gas emission from combustion products. This reliance on fossil-based fuel leads to significant depletion of buried combustible geologic deposits (Chandrasekhar *et al.* 2015) and makes the global economy immensely vulnerable to the state of petroleum industry. Scientific endeavors are engaged in developing alternative energy sources to replace fossil fuel. Among these alternatives, H_2 offers a tremendous potential as a clean and renewable energy currency. Unlike other alternative fuels, the combustion of H_2 produces water instead of CO_2 and other carbon-based emissions. H_2 energy yield (122 kJ/g) is greater

*Corresponding author: rgventura@up.edu.ph

than hydrocarbon (~40 kJ/kg) (Kapdan *et al.*2009) and holds the highest heating value (142 MJ/kg) among any other known fuels. Aside from satisfying the rising energy demand, hydrogen has many other industrial uses such as a reactant in hydrogenation processes, an O_2 scavenger that prevents the oxidation and corrosion of metallic materials, and a good coolant in electrical generators due to its unique physical property (Ramachandran and Menon 1998). To date, thirteen leading energy, transport, and related global industries intend to increase investment in the hydrogen and fuel sectors – which is currently at EUR 1.4 Bn/yr – to stimulate H_2 as a key part of the future energy mix via new policies and schemes (Stephen *et al.* 2017).

Currently, a large portion of the H_2 demand is being supplied from natural gas, by oil reforming, and by coal gasification (Arregi *et al.* 2018). These processes are taken from non-renewable resources and entail high production cost due to energy intensive operations. On the contrary, H_2 may be produced through biological systems that can operate at normal atmospheric pressures and relatively lower temperatures (30–55 °C) (Jarunglumlert *et al.* 2017). These approaches are more generally known as biohydrogen (Bio-H_2) production and offer a more environmentally benign and sustainable alternatives.

Biohydrogen can be produced through biophotolysis, microbial electrolysis (MEC), photofermentation, and dark fermentation. Biophotolysis is carried using photoautotrophic organisms like cyanobacteria and microalgae that use light energy to convert water to hydrogen (Rahman *et al.* 2015). MEC produces H_2 from the conversion of organic substrates under applied external potential (Liu *et al.* 2005). Dark fermentation – on the other hand – involves conversion of substrates by a group of anaerobic bacteria such as *Clostridium*, *Enterobacter,* and *Bacillus,* which are grown in the dark (Lukajtis *et al.* 2018). Hydrogen yield by dark fermentation is dictated by several factors such as substrate used, media composition, type of reactor, media pH, hydraulic retention time, among others. The effect of operating temperature has also been shown to vary depending on the type of inoculum used. Mesophilic and thermophilic bacteria have optimal growths at 30–45 °C and 50–60 °C, respectively.

Photofermentation, is carried using purple non-sulfur bacteria (PNSB) like *Rhodobacter sphaeroides*, *Rhodobacter capsulatus*, *Rhodovulum sulfidophilum*, and *Rhodopseudomonas palustris.* These organisms possess the capacity to photoheterotrophically convert organic acids into H_2 and CO_2. Since sustained biohydrogen production through dark fermentation is limited by end-product toxicity and acidification of the medium brought by organic acids (Stephen *et al.* 2017), PNSB may be utilized to further H_2 production of carbon-rich byproducts of dark fermentation.

PNSB has been widely known for their metabolic versatility (Hädicke *et al.* 2011). Their ability to use wide spectral light energy – as well as the capacity to consume a variety of organic compounds such as organic acids (Sagnak and Kargi 2011), amino acids (Xiao *et al.* 2014), simple sugars (Abo-Hashesh *et al.* 2013), glycerol (Ghosh *et al.* 2012), and ethanol (Liu *et al.* 2015) – makes them ideal for coupled wastewater treatment - energy production technology.

Aside from hydrogenase, PNSB also possess nitrogenase that catalyzes the fixation of N_2 – thereby producing H_2 as by-product. In the absence of N_2, however, the enzyme exclusively reduces protons (Ryu *et al.* 2014) to yield maximal H_2 production. Since photofermentation does not solely depend on hydrogenase to produce H_2, PNSB give sustained H_2 production even under an atmosphere of 100% H_2 gas (Kars and Gündüz 2010). Furthermore, PNSB theoretically produces only CO_2 and H_2 from the reduction of organic acids (Sasikala *et al.* 1990). This is in contrary to dark fermentation that produces H_2, CO_2, and lesser amounts of CO, CH_4, and/or H_2S in the final gas product (Rahman *et al.* 2015). Hence, purification of photofermentation gas product may only involve the separation of H_2 from CO_2.

Maintenance and creation of anaerobicity is among the factors that increase the cost of operation in bio-H_2 production systems. Sparging of reactor headspace during dark and photofermentation is done using Ar and N_2. Among the two, N_2 is widely used in dark fermentation reactors especially since N_2 is cheaper than Ar. Bioreactors in photofermentation, on the other hand, uses N_2 in gas sparging to avoid N_2-fixing condition. Not many literatures explore the possible use of N_2 in a photofermentation setup. In an investigation by Huang *et al.* (2010), *R. palustris* was pre-grown in N_2-fixing condition and harvested during mid-growth. The resulting non-growing cell suspensions were found to produce H_2 under Ar headspace, with thiosulfate and $NaHCO_3$ as electron donor and carbon source.

R. sphaeroides KCTC 1434 was shown to produce significant amount of H_2 from propionate and butyrate under Ar-rich headspace (Ventura *et al.* 2016). The presence of N_2 in the reactors resulted to decreased H_2 production but higher cell growth rate. This demonstrated that the strain fixed N_2 for cell growth, hence the minimal amount of H_2 produced. Investigation has been extended in this study to determine the effect of an alternating headspace gas replacement during the onset of H_2 production using propionate and butyrate as substrates during photofermentation. A report by Madigan *et al.* (1984) showed that among the species of *Rhodospirillaceae*, *R. sphaeroides* exhibited rapid growth and highest *in vivo* nitrogenase activity in a nitrogen-rich environment. Hence, this study would like to demonstrate

(1) if inhibition of N_2-fixing condition on H_2 production is reversible, (2) maintenance of N_2 headspace gas before the initiation of H_2 evolution might bring a higher cell growth rate and strong nitrogenase activity, and (3) subsequent replacement to an Ar-rich headspace will provide the enriched cells a higher capacity to produce H_2 gas. The reverse of this scenario was likewise carried to determine the physiological manifestations of N_2 fixation during the onset of H_2 production. This study may provide useful data for the possible utilization of N_2 in photofermentation reactors.

MATERIALS AND METHODS

Rhodobacter Strain and Pre-activation

PNSB, *Rhodobacter sphaeroides* KCTC 1434, was obtained from Korean Collection for Type Culture (KCTC). The organism was first streaked on Van Niel's (VN) agar medium and grown inside an anaerobic glove box (COY Laboratory Products Inc., Grass Lake, MI, USA) equipped with white LED (4k lux). The anaerobic box has a gas mixture of 5% H_2, 5% CO_2, and 90% N_2 and maintained at 30 °C during cultivation. Verified colonies grown on agar plates were then collected and transferred to serum bottles containing 60 mL of VN liquid medium (without agar). The liquid cultures were grown in a shaking incubator at 30 ± 1 °C and 120 ± 2 rpm under blue LED lamp for 24 h (Ventura *et al.* 2016). The cells from these cultures were harvested by centrifugation (4720 x *g*; Mega 17R, Hanil Science Industrial Co., Korea) for 10 min at 4 °C. The collected pellets were then washed with and resuspended in modified Pfennig & Bieble's medium (MPB) for preactivation.

The MPB media had the following basal composition: $MgSO_4{\cdot}7H_2O$ (0.2 g/L), NaCl (0.4 g/L), yeast extract (0.4 g/L), KH_2PO_4 (0.5 g/L), $CaCl_2{\cdot}2H_2O$ (0.05 g/L), ferric citrate ($5x10^{-3}$ g/L), $ZnCl_2$ (0.07 mg/L), H_3BO_3 (0.06 mg/L), $MnCl_2{\cdot}4H_2O$ (0.1 mg/L), $CoCl_2{\cdot}2H_2O$ (0.2 mg/L), $CuCl_2{\cdot}2H_2O$ (0.02 mg/L), $NiCl_2{\cdot}6H_2O$ (0.02 mg/L), $(NH_4)_2MoO_4{\cdot}2H_2O$ (0.04 mg/L), and HCl (0.025% v/v). The main carbon and nitrogen source used during preactivation were malic acid (7.5 mM) and sodium glutamate (10 mM), respectively. Moreover, a vitamin solution was added to better promote growth of the cultures. The vitamin solution had the following composition: nicotinic acid (0.2 mg/L), nicotinamide (0.2 mg/L), thiamine HCl (0.4 mg/L), and biotin (8.0 mg/L). The medium was flushed with N_2 gas for 10 min to ensure anaerobicity and the pH adjusted to pH 6.8 ± 1 using 5 M NaOH before autoclaving.

H_2 Production

After 24 h of preactivation, cells were collected from the preactivation media and were washed twice with MPB basal solution. The cells were then transferred to 160 mL serum bottles (Wheaton) containing 60 mL MPB H_2 production media. The MPB H_2 production medium was similar to the preactivation medium except for the carbon source and amount of glutamate used. H_2 production was carried using butyrate (15 mM) or propionate (20 mM) instead of malic acid. Butyrate and propionate concentrations were made proportional to the number of carbon atoms in each acid – based on the method of Uyar *et al.* (2009). Sodium glutamate was reduced to 2 mM as optimized elsewhere (Eroglu *et al.* 1999). Similarly, the medium pH was adjusted to pH 6.8 at the start of the experiments.

H_2 production was carried in two batches – each batch comprising of 4 reactors with propionate and another 4 reactors with butyrate as substrate. In the first batch of H_2 production, eight reactors were initially sparged with Ar. Sixty hours later, four of the Ar-sparged reactors (two propionate-fed and two butyrate-fed reactors) were repurged with N_2 to replace the initial Ar headspace gas. The remaining reactors were kept under Ar headspace throughout the duration of the experiment to serve as control. Treatments were designated as propionate N_2-repurged (PN_2R) and butyrate N_2-repurged (BN_2R). The change in H_2 production was compared against controls – propionate Ar-maintained (PArM), and butyrate Ar-maintained (BArM).

A reversal of the first set-up was carried in the second batch of the experiment where reactors were initially purged with N_2 and were later (after 60 h) repurged with Ar. The treatments were designated as propionate Ar-repurged (PArR) and butyrate Ar-repurged (BArR), which corresponded to the propionate- and butyrate-fed reactors that started with N_2 headspace and were later replaced with Ar. Controls were likewise kept under N_2 headspace through the entire duration and were designated as propionate N_2-maintained (PN_2M) and butyrate N_2-maintained (BN_2M). The 60 h repurging time corresponded to a linear increase in both cell density and hydrogen production, as determined by preliminary experiments (Ventura *et al.* 2016).

To ensure anaerobicity, purging of the reactor headspaces was done for 10 min in all experiments. The pressure in the serum bottles was released through a tube connected to an acidified brine solution. The cultures were incubated at 30 ± 1 °C, 120 ± 2 rpm, and illuminated in blue LED lamp.

Analytical Methods

A gas-tight glass syringe (Hamilton Co., Reno, NV, USA) was used to collect the gas samples from the reactor headspace and the biogas composition was analyzed using GC (HP 6890 Series, Agilent Technologies, USA) equipped with ShinCarbon ST 100/120 micropacked (cat.

#19808) column and a thermal conductivity detector. The pressure in the bioreactors was measured using a pressure sensor (SIKA D-53695, Germany) and was converted into volume using the method described in the previous paper (Ventura *et al.* 2016). The resulting volumes were multiplied with the percent gas composition from GC analysis to give the volume of H_2 gas generated. The pH of the culture media was measured using pH meter (Orion 290, CA, USA).

The concentration of propionate and butyrate was analyzed after adding formic acid and 2-ethylbutyrate using GC (HP 6890 Series, Agilent Technologies, USA) with a flame ionization detector and a capillary column (PB-FFAP, 0.25 µm, J & W Scientific, Folsom, CA, USA). Likewise, bacterial growth was monitored by measuring optical density at 660 nm using UV-Vis spectrophotometer (UV-1601PC, Shimadzu, Japan). Cell dry weight (DCW) was obtained using a standard curve where one unit of optical density corresponded to 0.27 ± 0.06 g DCW/L medium. All values were reported as ± standard deviation between each replicate.

Kinetic Model Analysis and Other Indicators

Kinetic parameters describing the H_2 production from each batch run were obtained using modified Gompertz equation (Equation 1):

$$H = P \exp\left\{-\exp\left[\frac{R_m e}{P}(\lambda - t) + 1\right]\right\} \quad (1)$$

where H is the cumulative H_2 production in mL, P the H_2 production potential in mL, R_m the maximum H_2 production rate in mL/h, λ the lag phase time, and t the incubation time. The values were determined by best fitting the H_2 production experimental data for Eq. 1 using the solver function (Newtonian algorithm) in Microsoft Excel Office 365 (Microsoft Corp., Redmond, WA, USA).

Specific growth rate was calculated over time intervals where cell density increased linearly with time using Equation 2:

$$\mu_{max} = \frac{\ln\frac{x_2}{x_1}}{t_2 - t_1} \quad (2)$$

where μ_{max} is the specific growth rate and x_1 and x_2 are cell densities at two different time points in the exponential phase (t_1 and t_2). The H_2 production potential is the cumulative H_2. Hydrogen yield (mol/mol) is equal to cumulative volume of H_2 produced converted into moles and divided by the amount of substrate consumed. Substrate consumption is the difference between the initial and final amount of substrate during the H_2 production experiment. Substrate conversion efficiency (SCE) is calculated by dividing the actual moles of H_2 produced with the computed H_2 equivalence of the consumed substrate (in moles).

The significant difference in cumulative H_2 production, DCW, and substrate consumption of the different systems was determined using one-way ANOVA, followed by the Bonferroni *t*-test for the pairwise comparison. Prior to the proper *t*-test analysis, an *F*-test was conducted to determine the variances (equal or unequal) of the two systems. A *p*-value of ≤ 0.05 or $\alpha = 0.05$ was considered statistically significant except for the two-tail *p*-value of the *t*-test to account for the multiple comparisons using Bonferroni's correction. In this case, the Bonferrroni's corrected test specific significance level for the comparison of four treatments is equal to 0.0125 (*i.e.*, $\alpha/4$). The data were analyzed using the Microsoft Office 365 data analysis tool.

RESULTS AND DISCUSSION

Effect of N_2 Replacement on Hydrogen Productivity in Ar-purged Propionate and Butyrate Reactors

Figure 1 shows the cumulative H_2 production in PN_2R (propionate, N_2-repurged) and BN_2R (butyrate, N_2-repurged) against PArM (propionate, Ar-maintained) and BArM (butyrate, Ar-maintained). During the first 60 h in which all reactors were under Ar headspace, average cumulative H_2 volumes of 35.1 ± 0.9 and 23.5 ± 1 mL were produced from butyrate and propionate, respectively. An immediate decrease in H_2 production on both acids was observed after N_2 replacement, with 42.4 ± 1.0 mL H_2 accumulation in BN_2R and 27.4 ± 0.2 mL H_2 accumulation in PN_2R until 348 h.

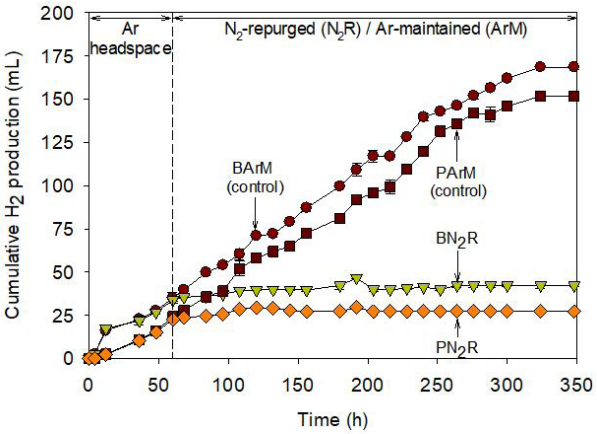

Figure 1. Cumulative H_2 production from propionate and butyrate under Ar-maintained and N_2-repurged headspace condition.

On the contrary, argon-maintained reactors gave sustained H_2 production until 348 h at 168.59 ± 1.14 and 151.80 ± 1.25 mL H_2 in BArM and PArM, respectively. The observed difference in cumulative H_2 between PArM and PN_2R (p Critical two-tail = 2.93 x 10^{-5} > 0.0125), and BArM and BN_2R (p Critical two-tail = 4.74 x 10^{-5}) were significantly different. This conforms to the fact that N_2 fixation and biohydrogen production are two processes that compete for the reducing equivalent in cells. Except for some metabolism studies that make use of flux balance analysis to indicate reductant distributions in PNSB (Golomysova *et al.* 2010, Hadicke *et al.* 2011); a few is written on how this competition between N_2 fixation and H_2 production is being manifested physiologically.

To further describe the H_2 production under changing headspace gas composition, modified Gompertz fitting was carried with the resulting kinetic parameters shown in Table 1. The maximum production rate (R_m) values of PN_2R and BN_2R were 0.37 and 0.52 mL H_2/h, respectively. Hence, there was none or minimal H_2 production from the two acid substrates in the presence of N_2. H_2 production lag time values were determined to be 4 h in all reactors except for BN_2R, where λ is 0. All reactors were therefore in the exponential phase of H_2 production (under the initial Ar headspace) when N_2 replacement was carried in PN_2R and BN_2R. The occurrence of N_2 inhibition at 60 h was therefore manifested in PN_2R and BN_2R.

Lower H_2 yields were observed in N_2-repurged reactors (1.43 and 2.69 in PN_2R and BN_2R, respectively). The SCE values in PN_2R (20.49%) and BN_2R (26.89%) were 4.5 and 3.5 times lower than Ar-maintained reactors. It is therefore evident that under Ar headspace, a large part of the propionate and butyrate consumed has been utilized for hydrogen production rather than growth or alternative biosynthesis (Sasikala *et al.* 1993).

Figure 2A and Figure 2B illustrate the effect of N_2 replacement on cell density and substrate consumption in propionate and butyrate. There was almost no growth lag time observed in the two acids under the initial Ar

Table 1. Kinetic parameters from modified Gompertz analysis, H_2 yield, SCE, and final pH during H_2 production from propionate and butyrate under Ar-maintained and N_2-repurged headspace conditions.

Condition	Substrate	Kinetic Parameters				H_2 Yield (mol H_2/mol substrate consumed)	SCE[d] (%)	Final pH
		P[a] (mL H_2 produced)	R_m[b] (slope)	λ[c] (lag time)	R^2			
Ar-maintained	Propionate	151.80	0.54	4	0.997	6.43	91.83	8.0
	Butyrate	168.59	0.56	4	0.996	9.40	94.03	7.8
N_2-repurged	Propionate	27.36	0.37	4	0.993	1.43	20.49	11.0
	Butyrate	42.24	0.52	0	0.994	2.69	26.89	12.0

Notes:
[a]H_2 production potential
[b]Highest H_2 production rate
[c]H_2 production lag time
[d]Substrate conversion efficiency

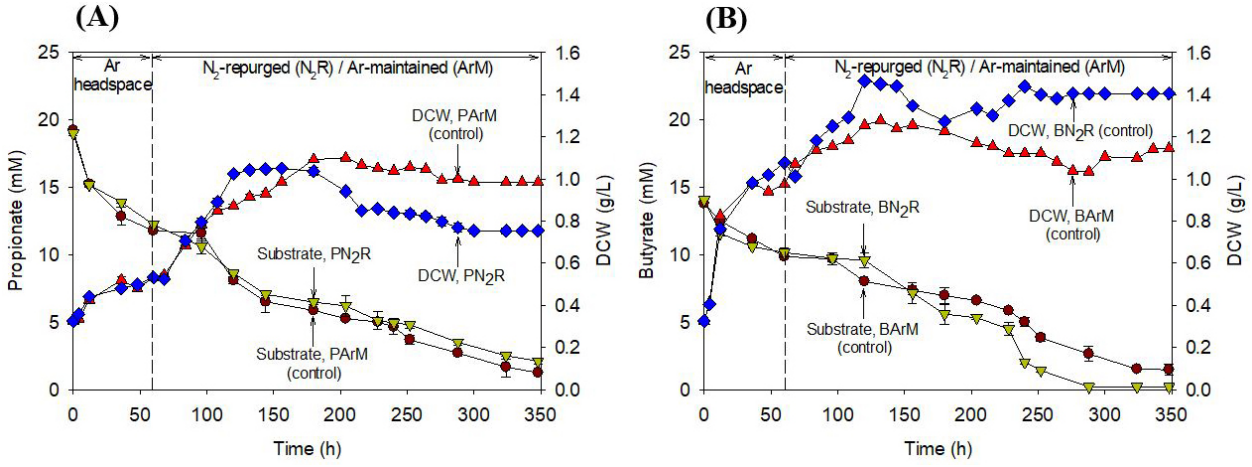

Figure 2. Substrate consumption and cell growth in (a) propionate and (b) butyrate during H_2 production under Ar-maintained and N_2-repurged headspace condition.

headspace (0–60 h). This corresponded to cell densities averaging 0.482 ± 0.000 (specific growth rate = 0.008 ± 0.000) and 0.928 ± 0.066 g/L (specific growth rate = 0.019 ± 0.001 h^{-1}) for propionate and butyrate, respectively. Immediately after replacing Ar with N_2, the cell density in PN_2R started to rise such that – at the end of 120 h – PN_2R had cell density 1.2 times higher than PArM. A similar rise in DCW was also observed in BN_2R. In 120 h, BN_2R and BArM had maximum cell densities of 1.33 ± 0.02 and 1.14 ± 0.02 g/L, respectively. Corresponding specific growth rates were determined to be 0.005 (for PN_2R) and 0.011 h^{-1} (for BN_2R). While ANOVA showed variations among the obtained DCW ($p = 6.01 \times 10^{-10}$), subsequent *post-hoc t*-test results indicated that the cell density differences in PArM and PN_2R (p Critical two-tail = 0.2299 > 0.0125) and in BArM and BN_2R (p Critical two-tail = 0.0310 > 0.0125) were not significant.

ANOVA results gave no significant differences in substrate consumption at p-value equal to 0.09427. In propionate-fed reactors, an average substrate consumption rate of 0.107 ± 0.011 mM h^{-1} was observed under the initial Ar headspace. After N_2 replacement, a consumption rate of 0.038 mM h^{-1} was measured in PN_2R, which did not vary remarkably from PArM (0.037 mM h^{-1}). Hence, N_2 replacement in PN_2R did not affect propionate consumption rate. In butyrate-fed reactors, the average substrate consumption rate of BArM was 0.061 ± 0.004 mM h^{-1}, while 0.046 ± 0.016 mM h^{-1} butyrate was consumed in BN_2R. Hence, it can be observed that propionate and butyrate consumption rates were not affected by the replacement of Ar headspace gas with N_2. Sasikala *et al.* (1990) did not include cell growth in their report, but their investigation on *R. sphaeroides* O.U. 001 showed that – although there was no H_2 production under N_2 gas phase – there was no substantial difference in the percent malate consumption under Ar and N_2 headspace gases.

It is therefore apparent that N_2-fixation automatically hinders maximal H_2 production in both PN_2M and BN_2M. The very minimal H_2 observed in PN_2M and BN_2M may have been H_2 expelled as a side product of bacterial growth, which was higher under N_2 headspace.

Effect of Ar Replacement on Hydrogen Productivity in N_2-purged Propionate and Butyrate Reactors

In the second batch, reactor headspaces were initially purged with N_2. While duplicate controls were kept unchanged under N_2 headspace, the other set was repurged with Ar after 60 h. Treatments were designated as PArR (propionate Ar-repurged) and BArR (butyrate Ar-repurged) and were compared with the controls – namely PN_2M (propionate N_2-maintained) and BN_2M (butyrate N_2-maintained).

Replacing Ar with N_2 in the previous run instantly decreased the amount of H_2 produced from propionate and butyrate. In the second run, replacing N_2 with Ar did not show immediate surge of H_2 production from both acids (Figure 3).

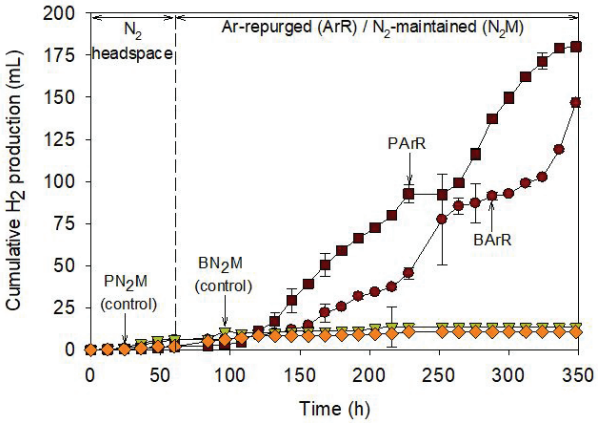

Figure 3. Cumulative H_2 production from propionate and butyrate under N_2-maintained and Ar-repurged headspace condition.

During the first 60 h under N_2 headspace, propionate- and butyrate-fed reactors evolved an average of 1.93 ± 0.01 and 5.99 ± 0.21 mL H_2, respectively. At 156 h (96 h after N_2 repurging), PArR accumulated 37.41 ± 2.14 mL H_2 and BArR produced 8.72 ± 0.77 mL H_2. At 348 h, volumes of 180.05 ± 1.30, 146.68 ± 2.79, 10.65 ± 0.53, and 13.50 ± 1.06 mL H_2 were accumulated in PArR, BArR, PN_2M, and BN_2M, respectively. The very low cumulative H_2 in N_2-maintained reactors were found significantly different (PN_2M *vs.* PArR: p Critical two-tail = 2.30×10^{-4}; BN2M *vs.* BArR: p Critical two-tail = 1.03×10^{-5}) from the argon-repurged reactors.

Modified Gompertz fitting was conducted to determine kinetic parameters to describe the overall H_2 production in this batch run (Table 2). The λ values of 144 and 172 h, respectively, were determined for PArR and BArR. These corresponded to 84 (in PArR) and 112 hours (in BArR) after the Ar-repurging time. The long lag time of PArR and BArR after Ar-repurging may be attributed to the accumulation of NH_3, which may have been consumed just before H_2 production started to surge. In a study conducted by Kim *et al*. (2012a), longer lag time was observed in *R. sphaeroides* KD131 grown in succinate – with ammonium sulfate as N source – compared to glutamate. Lower nitrogenase activity was observed with ammonium (15 and 303 nmol/g DCW/h in ammonium sulfate and glutamate, respectively) during the initial hours and a gradual increase was exhibited upon the depletion of NH_4^+ (Kim *et al.* 2012b).

Table 2. Kinetic parameters from modified Gompertz analysis, H_2 yield, SCE, and final pH during H_2 production from propionate and butyrate under N_2-maintained and Ar-repurged headspace conditions.

Condition	Substrate	Kinetic Parameters				H_2 Yield (mol H_2/mol substrate consumed)	SCE[d] (%)	Final pH
		P[a] (mL H_2 produced)	R_m [b] (slope)	λ[c] (lag time)	R^2			
Ar-repurged	Propionate	180.05	1.05	144	0.988	6.95	96.63	8.2
	Butyrate	146.68	0.67	172	0.987	5.64	56.50	9.0
N_2-maintained	Propionate	10.65	0.08	24	0.990	0.76	10.90	10.8
	Butyrate	13.50	0.09	0	0.983	1.36	13.61	11.1

Notes:
[a]H_2 production potential
[b]Highest H_2 production rate
[c]H_2 production lag time
[d]Substrate conversion efficiency

H_2 production rate of 1.05 mL H_2/h was determined from PArR and 0.67 mL H_2/h from BArR. Remarkably, PArR exhibited a higher H_2 production than BArR. While PN_2R and BN_2R gave hydrogen production rates of 0.54 and 0.56 mL H_2/h (Table 1), PArR and BArR gave higher H_2 production rates at 1.05 and 0.67 mL H_2/h, respectively.

Ar-replacement of the initial N_2 headspace, however, gave variable effects on SCE of the two acid substrates. While PArR gave an SCE value (96.63%) higher than the other propionate reactors under Ar headspace (PArM), BArR had an SCE value (56.50%) markedly smaller than the other argon-purged butyrate reactors (BArM). The N_2-fixing to non N_2-fixing condition may have therefore enhanced the conversion efficiency of propionate but not of butyrate. The hydrogen production rate and the SCE values may suggest that, although butyrate is capable of producing H_2, it may also be used for an alternative biosynthetic pathway given a certain physiological condition. In the investigation of Pandey *et al.* (2012), H_2 production of *R. sphaeroides* NMBL-01 on butyrate gave an SCE of 14.1% – with lactate and PHB as end metabolites. Metabolic-flux studies (Golomysova *et al.* 2010, Rey *et al.* 2007) have identified three pathways that compete for electrons during H_2 productions – namely CO_2 fixation, N_2 fixation, and polyhydroxybutyrate (PHB) biosynthesis. Although investigation for PHB production was not included in the scope of this study, this biosynthetic pathway could possibly account for the low H_2 production in BArR reactors.

ANOVA of DCW in PArR, BArR, PN_2M, and BN_2M showed variations at $p = 7.87 \times 10^{-10}$. Subsequent *post-hoc t*-test showed that the difference in cell densities between PN_2M and PArR (p Critical two-tail = 0.0058 < 0.0125) and BN_2M and BAr (p Critical two-tail = $6.81 \times 10^{-5} < 0.0125$) were significant. Moreover, as observed in Figures 4A and 4B, placing the reactors under N_2 headspace followed by Ar repurging has brought a relatively longer exponential phase on cell growth of *R. sphaeroides*. The cell density in PArR continued to rise to 1.03 ± 0.017 g h^{-1} until the 288 h, giving a specific growth rate (0.003 h^{-1}) that was twice higher than PN_2M. Likewise BArR exhibited a linear increase in cell density with a specific growth rate of 0.003 h^{-1} until 348 h, while BN_2M cell density curve has started to level off. From Figure 2, this duration where a linear increase in cell density was observed also corresponded to a stable production of H_2. Compared to PArM and BArM in the first experimental set-up, PArR and BArR had an apparently longer exponential phase that extends beyond 200 h. While the argon-maintained reactors had hydrogen production that peaked beyond the stationary phase of bacterial cell growth, the H_2 production of PArR and BArR occur along the exponential phase on the bacterial cell density curve. Investigations have been made on H_2 production by PNSB using growing (Hillmer and Gest 1977a) and resting cells (Hillmer and Gest 1977b). Resting cells are harvested at stationary phase of growth. These possess live nitrogenase enzymes and can therefore carry H_2 production. In the investigation of Melnicki *et al.* (2008), resting cells of *R. rubrum* UR2 and *R. palustris* CG A009 showed diminishing H_2 production ability despite successive succinate replenishment. Their study suggested that although H_2 production is not necessarily coupled with cell growth, growth is important in order to obtain maximal hydrogen production rates. Physiological events such as diminished bioenergetic activity, storage polymer accumulation, and gradual loss of cell vitality and viability accompany the stationary phase of bacterial cell growth (Nystrom 2004).

Several factors could lead cells to enter the stationary phase. Among these, nutrient limitation is one major cause. There is no clear explanation on the delayed stationary phase in PArR and BArR, although it may be thought that glutamate could be conserved when N_2 is present. Since nitrogenase has higher affinity to N_2, fixation occurs inevitably (Koku *et al.* 2002). It is possible that during the initial hours under

N_2 headspace, amino acid precursors were supplied from NH_3 produced from the enzymatic N_2 reduction. In a study using a mixture of ammonia and L-glutamate as nitrogen source, several nitrogen-fixing rhizobia were found to preferentially use ammonia by repressing the synthesis of L-glutamate transport system (Poole *et al.* 1987). It is not however known whether this mechanism holds true in PNSB. However, the minimal H_2 production under N_2 headspace and the long lag time after Ar-repurging suggest an elevated N status in PArR and BArR – possibly due to unconsumed glutamate and NH_4^+. The metabolism of *R. sphaeroides* shifts to cell synthesis in the presence of high N_2 concentration and H_2 production is only recovered after ammonia is consumed (Kirtay 2011).

ANOVA indicated variations in substrate consumptions (Figure 4) of the reactors at $p = 0.0009$. *Post-hoc t*-test, however, showed that the differences in substrate consumption between PArR and BArR (p Critical two-tail = 0.9087 > 0.0125), PArR and BN_2M (p Critical two-tail = 0.1242 > 0.0125), and BArR and BN_2M (p Critical two-tail = 0.0390 > 0.0125) are not statistically different. Corresponding substrate consumption rates were 0.050, 0.050, 0.022, and 0.011 mm h^{-1} in PaR, BaR, PN_2M, and BN_2M, respectively. This observation may have been brought about by the high energy expending nature of nitrogenase. In the absence of its natural substrate (N_2), the enzyme catalyzes hydrogen production in an ATP-dependent manner (Rey *et al.* 2007) as depicted in Equation 4:

$$N_2 + 8e^- + 8H^+ + 16ATP \rightarrow 2NH_3 + H_2 + 16ADP \quad (3)$$

$$8e^- + 8H^+ + 16ATP \rightarrow 4H_2 + 16ADP \quad (4)$$

Additionally, N_2-maintained reactors exhibited higher final pH (10.8 in PN_2M and 11.1 in BN_2M, Table 2) than the Ar-repurged reactors (pH 8.2 in PArR and pH 9.0 in BArR). Similar to the first set-up, reactors that were under N_2 headspace (PN_2R and BN_2R) had final pH that were markedly higher than their Ar-maintained counterparts (Table 1).

The difference in SCE of PArR and BArR (Table 2) may be attributed to the effect of pH on H_2 production. pH was observed to be higher in BArR (pH = 8) than in PArR (pH = 7) prior to Ar repurging (0–60 h, data not shown). This difference during the 60 h headspace replacement was not observed in Ar-purged reactors in the first experimental set-up. PArM, PN_2R, BArM, and BN_2R had pH values that were around pH 7 at 60 h (N_2-repurging). It may also be noted that in Table 2, BArR showed longer H_2 production lag time than PArR. An initial pH of 7.0 ± 0.2 has been suggested in several studies (Fang *et al.* 2005, Kim *et al.* 2012a, Yang *et al.* 2014) as the best value for H_2 production in *R. sphaeroides* strains.

From the theoretical stoichiometry of nitrogenase (Eq. 3) NH_3 is produced when N_2 is reduced, and ammonium ion inhibits H_2-producing activity (Sasikala *et al.* 1990; Khatipov *et al.* 1998; Koku *et al.* 2002; Kim *et al.* 2012a, 2012b). The increased pH in the presence of N_2 may have been due to the accumulation of ammonia in the reactors. Lactate-grown *R. sphaeroides* RV gave higher pH with 10mM NH_4^+ than with 10 mM glutamate as N source (Khatipov *et al.* 1998). In an investigation conducted by Kim *et al.* (2012a), *R. sphaeroides* KD131 gave a higher final pH in 30 mM succinate/4 mM $(NH_4)_2SO_4$ than in 20 mM succinate/8 mM glutamate.

CONCLUSION

Propionate and butyrate provided substantial amount of H_2 under Ar headspace, while the presence of N_2 manifested a reversible inhibition of H_2 production. The replacement of Ar headspace gas with N_2 along the exponential period of H_2 production immediately decreased H_2 evolution,

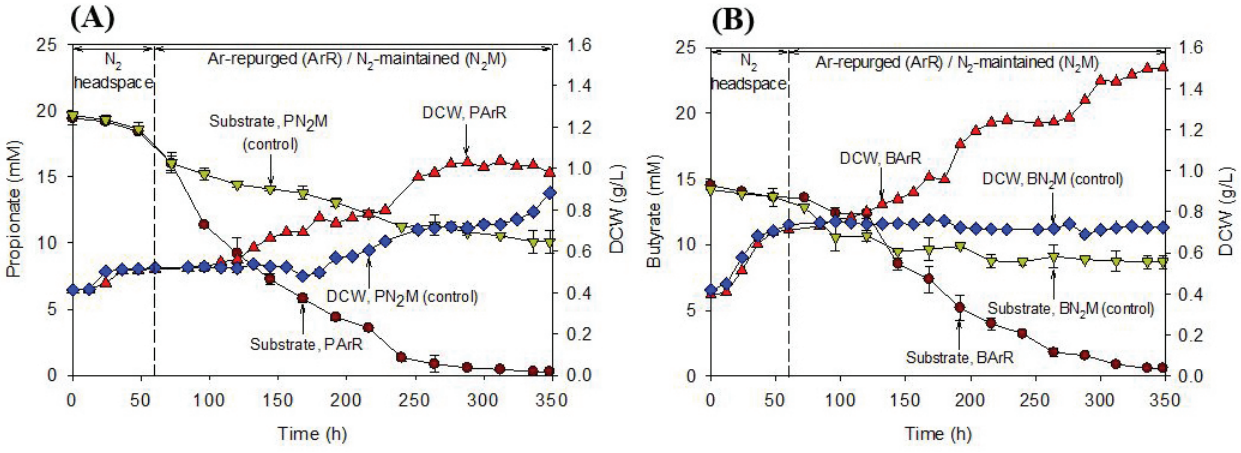

Figure 4. Substrate consumption and cell growth in (a) propionate and (b) butyrate during H_2 production under N_2-maintained and Ar-repurged headspace condition.

suggesting an inhibition by nitrogen fixation. PArR and BArR reactors showed better hydrogen production rate (R_m), although only propionate obtained a relatively higher SCE (96.63%) after repurging with Ar.

No significant difference among substrate consumption was observed in any of the investigated headspace gases. This result shows that nitrogenase-mediated reaction is ideal for the consumption of organic acids in wastewater.

Notably, placing the reactors under N_2 and later replacing the gas with Ar brought significantly higher cell densities on propionate and butyrate with an apparently prolonged growth phase of *R. sphaeroides* KCTC 1434. This suggests that the N_2-to-Ar scheme simulated a condition wherein bacterial cells were enhanced to allow a stable and maximum H_2 production without altering genetic makeup. Stronger evidence of N_2-fixation may be supported with the analysis of NH_3 and PHB in the system.

Overall, there is no significant difference (p = 0.0943) in the cumulative hydrogen production between Ar-maintained and Ar-repurged cultures. However, since high pH impacts negatively on H_2 production, additional studies using pH-controlled conditions may be implored to further improve H_2 productivity.

This investigation shows that the use of N_2-to-Ar scheme, as suggested, may be feasible during photofermentative hydrogen production. Further exploration in this line may offer opportunity in reducing operation cost, particularly in the use of gas for sparging photofermentation reactors.

ACKNOWLEDGMENTS

This research was supported by the Basic Science Research Program through the National Research Foundation of Korea (NRF) – funded by South Korea's Ministry of Education, Science and Technology.

REFERENCES

ABO-HASHESH M, DESAUNAY N, HALLENBECK PC. 2013. High yield single state conversion of glucose to hydrogen by photofermentation with continuous culture of *Rhodobacter capsulatus* JP91. Bioresource Technology 128: 513–517.

ARREGI A, AMUTIO M, LOPEZ G, BILBAO J, OLAZAR M. 2018. Evaluation of thermochemical routes for hydrogen production from biomass: A review. Energy Conversion and Management 165: 696–719.

CHANDRASEKHAR K, LEE Y-J, LEE D-W. 2015. Biohydrogen Production: Strategies to Improve Process Efficiency through Microbial Routes. International Journal of Molecular Sciences 16(4): 8266–93.

EROGLU I, ASLAN K, GÜNDÜZ U, YÜCEL M. TÜRKER L. 1999. Substrate consumption rates for hydrogen production by *Rhodobacter sphaeroides* in a column photobioreactor. Journal of Biotechnology 70: 103–113.

FANG HHP, LIU H, ZHANG T. 2005. Phototrophic hydrogen production from acetate and butyrate in wastewater. International Journal of Hydrogen Energy 30: 785–793.

GOLOMYSOVA A, GOMELSKY M, IVANOV PS. 2010. Flux balance analysis of photoheterotrophic growth of purple nonsulfur bacteria relevant to biohydrogen production. International Journal of Hydrogen Energy 35: 12751–60.

GHOSH D, SOBRO IF, HALLENBECK PC. 2012. Stoichiometric conversion of biodiesel derived from crude glycerol to hydrogen: Response surface methodology study of the effects of light intensity and crude glycerol and glutamate concentration. Bioresource Technology 106: 154–160.

HÄDICKE O, GRAMMEL H, KLAMT S. 2011. Metabolic network modeling of redox balancing and biohydrogen production in purple nonsulfur bacteria. BMC Systems Biology 5: 150.

HILLMER P, GEST H. 1977a. H_2 Metabolism in the photosynthetic bacterium *Rhodopseudomonas capsulata*: H_2 production by growing cultures. Journal of Bacteriology 129(2): 724–731.

HILLMER P, GEST H. 1977b. H_2 metabolism in the photosynthetic bacterium *Rhodopseudomonas capsulata*: Production and utilization of H_2 by resting cells. Journal of Bacteriology 129(2): 732–739.

HUANG JJ, HEINIGER EK, McKINLAY JB, HARWOOD CS. 2010. Production of Hydrogen Gas from Light and the Inorganic Electron Donor Thiosulfate by *Rhodopseudomonas palustris*. Applied and Environmental Microbiology 76(23): 7717–22.

JARUNGLUMLERT T, PROMMUAK C, PUTMAI N, PAVASANT P. 2017. Scaling-up bio-hydrogen production from food waste: Feasibilities and challenges. International Journal of Hydrogen Energy 43: 634–648.

KAPDAN I, KARGI F, OZTEKIN R, ARGUN H. 2009. Bio-hydrogen production from acid hydrolyzed wheat starch by photo-fermentation using different *Rhodobacter sp*. International Journal of Hydrogen Energy 34: 2201–07.

KARS G, GÜNDÜZ U. 2010. Towards a super H_2 producer: Improvements in photofermentative biohydrogen production by genetic manipulations. International Journal of Hydrogen Energy 35: 6646–56.

KHATIPOV E, MIYAKE M, MIYAKE J, ASADA Y. 1998. Accumulation of poly-β-hydroxybutyrate by *Rhodobacter sphaeroides* on various carbon and nitrogen substrates. FEMS Microbiology Letters 162: 39–45.

KIM M, KIM D, CHA J. 2012a. Culture conditions affecting H_2 production by phototrophic bacterium *Rhodobacter sphaeroides* KD131. International Journal of Hydrogen Energy 37: 14055–61.

KIM M, KIM D, CHA J, LEE JK. 2012b. Effect of carbon and nitrogen sources on photo-fermentative H_2 production associated with nitrogenase, uptake hydrogenase activity, and PHB accumulation in *Rhodobacter sphaeroides* KD131. Bioresource Technology 116: 179–183.

KIRTAY E. 2011. Recent advances in production of hydrogen from biomass. Energy Conversion and Management 52: 1778–89.

KOKU H, EROĞLU İ, GÜNDÜZ U, YÜCEL M, TÜRKER L. 2002. Aspects of the metabolism of hydrogen production by *Rhodobacter sphaeroides*. International Journal of Hydrogen Energy 27: 1315–29.

LIU H, GROT S, LOGAN BE. 2005. Electrochemically assisted microbial production of hydrogen from acetate. Environmental Science and Technology 39: 4317–20.

LIU Y, GHOSH D, HALLENBECK PC. 2015. Biological reformation of ethanol to hydrogen by *Rhodopseudomonas palustris* CGA009. Bioresource Technology 102: 8557–68.

MADIGAN M, COS S, STEGEMAN R. 1984. Nitrogen fixation and nitrogenase activities in members of the family *Rhodospirillaceae*. Journal of Bacteriology 157(1): 73–78.

MELNICKI M, BIANCHI L, DE PHILIPPIS R, MELIS A. 2008. Hydrogen Production during the stationary phase in Purple Photosynthetic Bacteria. International Journal of Hydrogen Energy 33: 6525–34.

NYSTROM T. 2004. Stationary phase Physiology. Annual Review of Microbiology 58: 161–181.

PANDEY A, SRIVASTAVA N, SINH P. 2012. Optimization of hydrogen production by *Rhodobacter sphaeroides* NMBL-01. Biomass and Bioenergy 32: 251–256.

POOLE P, DILWORTH MJ, GLENN AR. 1987. Ammonia is the preferred nitrogen source in several rhizobia. Journal of General Microbiology 133: 1707–12.

RAHMAN SNA, MASDAR MS, ROSI MI, MAJLAN EH, HUSAINI T. 2015. Overview of Biohydrogen Production Technologies and Application in Fuel Cell. American Journal of Chemistry 5(3A): 13–23.

RAMACHANDRAN R, MENON RK. 1998. An overview of industrial uses of hydrogen. International Journal of Hydrogen Energy 23: 593–598.

REY F, HEINIGER E, HARWOOD C. 2007. Redirection of metabolism for biological hydrogen production. Appl. Environ. Microbiol. 73(5): 1665–71.

RYU M-H, HULL NC, GOMELSKY M. 2014. Metabolic engineering of *Rhodobacter sphaeroides* for improved hydrogen production. International Journal of Hydrogen Energy 39: 6384–90.

SAGNAK R, KARGI F. 2011. Photo-fermentative hydrogen gas production from dark fermentation effluent of acid hydrolyzed wheat starch with periodic feeding. International Journal of Hydrogen Energy 36: 4348–53.

SASIKALA K, RAMANA CV, RAGHUVEER RAO P, SUBRAHMANYAM M. 1990. Effect of gas phase on the photoproduction of hydrogen and substrate conversion efficiency in the photosynthetic bacterium *Rhodobacter sphaeroides* O.U. 001. International Journal of Hydrogen Energy 15: 795–797.

STEPHEN AJ, ARCHER SA, OROZCO RL, MACASJIE LE. 2017. Advances and bottlenecks in microbial hydrogen production 10(5): 1120–27.

UYAR B, EROGLU I, YŸCEL M, GŸNDŸZ U. 2009. Photofermentative hydrogen production from volatile fatty acids present in dark fermentation effluents. International Journal of Hydrogen Energy 34: 4517–23.

VENTURA RLG, VENTURA JS, OH Y-S. 2016. Investigation of the Photoheterotrophic Hydrogen Production of *Rhodobacter sphaeroides* KCTC 1434 using Volatile Fatty Acids under Argon and Nitrogen Headspace. American Journal of Environmental Sciences 12(6): 358–369.

XIAO N, CHEN Y, CHEN A, FENG L. 2014. Enhanced Bio-hydrogen Production from Protein Wastewater by Altering Protein Structure and Amino Acids Acidification Type. Scientific Reports 4: 3992.

YANG H, ZHANG J, WANG X, JIANGTAO F, YAN W, LIEJIN G. 2014. A newly isolated *Rhodobacter sphaeroides* with high hydrogen production performance. International Journal of Hydrogen Energy 39(19): 10051–60.